Title
BINDING BETWEEN CARBON ATOMS AND VACANCIES IN PLATINUM

Authors
Dahmen, U.
Westmacott, K.H.

Publication Date
1985-08-01

Lawrence Berkeley Laboratory
UNIVERSITY OF CALIFORNIA

Materials & Molecular Research Division

Presented at the International Seminar on
Solute-Defect Interactions, Kingston, Ontario,
August 5-9, 1985

BINDING BETWEEN CARBON ATOMS AND VACANCIES IN PLATINUM

U. Dahmen and K.H. Westmacott

August 1985

Prepared for the U.S. Department of Energy under Contract DE-AC03-76SF00098

DISCLAIMER

BINDING BETWEEN CARBON ATOMS AND VACANCIES IN PLATINUM

U. Dahmen and K.H. Westmacott

National Center for Electron Microscopy,
Materials and Molecular Research Division,
Lawrence Berkeley Laboratory,
University of California,
Berkeley, California 94720

ABSTRACT

Evidence for a large binding energy ($\gtrsim$0.5eV) between interstitially dissolved carbon atoms and vacancies has been obtained from three types of experiment on platinum. This paper reviews the evidence for the precipitation, diffusion and ordering of carbon atom/vacancy pairs and discusses some implications of strong vacancy/impurity binding.

KEYWORDS

Solute/vacancy binding; interstitial Pt-C alloy; precipitation sequence; coupled diffusion; order/disorder; electron irradiation; transmission electron microscopy; carbon solubility; vacancy supersaturation; impurity effects.

INTRODUCTION

Binding between solute atoms and vacancies is known to play an important role in diffusion, segregation and precipitation phenomena. Substitutional atom/vacancy interactions have been investigated in both fcc and bcc metals but until recently interstitial solute/vacancy binding has been studied only in bcc metals (1). The present paper presents and discusses some recent work on the binding between interstitial carbon and vacancies in an fcc metal.

The material used in the present work was nominally pure platinum with trace amounts (<800 at.ppm) of carbon. It was established that

a rapid quench from near the melting temperature in ultrahigh vacuum produced a high density of unusual faulted vacancy loops on {001} planes (2). These were found to arise from the co-precipitation of carbon atoms and vacancies. During subsequent annealing further intermediate precipitate phases developed and detailed investigation revealed their crystal structure and growth mechanisms (3,4). In studying the entire precipitation and dissolution sequences in this alloy it was concluded that at all stages vacancies played a crucial role in the nucleation and growth of the metastable carbide phase Pt_2C. The observations pointed to an unusually high carbon atom/vacancy binding energy, and both the structural and kinetic data suggested that carbon and vacancies diffuse, precipitate and disperse as bound complexes (5).

This lead to a new set of experiments in which it was shown that carbon diffusing through a thin Pt membrane causes a counterflow of Pt atoms, thus providing an independent confirmation of the binding hypothesis (6). Interestingly, the effect was enhanced near the grain boundaries, and further investigation revealed a large excess concentration of carbon near the boundaries.

Furthermore, it was found that under high-energy electron irradiation in a well-defined temperature interval a reversible order/disorder reaction could be induced (7). The ordered phase was consistent with a stoichiometry of Pt_7C, and again vacancies were crucial to its formation.

Most of the experimental work to be described here has been reported elsewhere (2-7); the present contribution is an attempt to

present a coherent picture of the diverse and unusual consequences, of carbon atom/vacancy interaction in platinum alloys. The evidence will be reviewed in three sections; part 1) summarizes the extensive observations on the sequence of carbon precipitation, part 2) reports the results of carbon diffusion experiments through platinum membranes and part 3) centers on in-situ experiments performed in a high voltage electron microscope in which an order/disorder reaction and precipitate growth and dissolution were observed.

1) The Effect of Carbon Atom/Vacancy Binding on Precipitation

Platinum foil containing about 800 at.ppm carbon was joule heated close to the melting point in ultrahigh vacuum and quenched by turning off the heating current. Fig. 1 shows TEM micrographs of the resulting microstructure, a high density of planar defects about 100nm in size located on {001} planes exhibiting displacement fringe and dislocation loop contrast. A contrast analysis, part of which is shown in Fig. 1a-c, determined the fault displacement vector $\underline{R}$ and dislocation Burgers vector $\underline{b}$ to be approximately $\pm$ a/3 <001>. For example in a 111 reflection the bounding dislocations are out of contrast ($\underline{g}.\underline{b} < 1/3$). On the other hand, a 311 reflection shows strong dislocation contrast ($\underline{g}.\underline{b} = 1$) and no displacement fringes ($\underline{g}.\underline{R}$ = integer) for one set of defects. Inside/outside contrast analysis revealed a displacement field of vacancy type. These features were consistent with the formation by a co-precipitation mechanism in which tightly bound carbon atom/vacancy pairs condensed and collapsed in an {001} planar disc. The structure of this precipitate was that of a single layer of carbon decorating and stabilizing an {001} stacking fault by filling the

interstices associated with the a-a stacking sequence at the fault. This stage of precipitation could be viewed as semicoherent GP zones of carbon and were designated α precipitates.

The second stage in the sequence (α') evolved during post-quench aging at 400°C. Fig. 2 shows the contrast behavior of α' precipitates in the same contrast analysis as shown for α above. The difference is clearly apparent in b) ($g=\bar{2}02$) where α' precipitates lack any displacement fringe contrast ($\underline{g}.\underline{R}$ = integer) and two variants show dislocation loop contrast ($\underline{g}.\underline{b}$ = 1). It was concluded that the displacement vector had increased to $\pm$ a/2 <001>, the nature of the displacement field still being of vacancy type. The α' plates were larger than α plates and their concentration considerably less.

At this stage it was possible to obtain microdiffraction patterns such as the one in Fig. 3a from single α' platelets in an edge-on orientation. The spots from the particle are marked by arrows. They are streaked due to the small thickness of the plate. The structure of the precipitate phase deduced from this and many other patterns is shown in Fig. 3b and is isomorphous with $\theta'Al_2Cu$. Its stoichiometric composition is Pt_2C.

Further post-quench aging in the temperature range 400-530° C resulted in coarsening and the appearance of α'' precipitates, the next stage in the precipitation sequence. As apparent from the contrast analysis in Fig. 4 (analogous to Figs. 1 and 2) these α'' precipitates are characterized by a vacancy type displacement field of a<001> and arise with the α' grows to two unit cell thickness.

Continued aging at temperatures above 500°C led to the formation of widely spaced and densely packed linear arrays of {001} plate precipitates unevenly distributed in the foil.

2. The Effect of Carbon Atom/Vacancy Binding on Diffusion

In order to explore the effect of carbon/vacancy interaction on the diffusion of carbon, Pt membranes were carburized on one side and decarburized on the other at temperatures between 700 and 900° C(6). As shown in SEM micrographs in Fig. 5, mounds appear on the inner, carburized side (b) and pits on the outer, decarburized side (a). The effect was enhanced at the grain boundaries but was also visible in the grain interiors. The pits and mounds were the result of vacancies diffusing in the same direction as the carbon atoms and giving rise to a counterflow of Pt atoms. An estimate of $\sim$0.5eV was obtained for the binding energy on the basis of the measured mound and pit volume assuming a steady state flux of carbon atoms calculated from Fick's law and a corresponding flux of carbon atom/vacancy pairs given by Lomer's equation. A similar though less accurate estimate of 0.5 to 0.6eV was made by comparing measured numbers of vacancies and carbon atoms transported.

From these data it was concluded that at 900°C about 1% of the carbon atoms traversing the foil are bound to vacancies. Surprisingly, a large number of vacancies are transported through, or adjacent to, the boundaries even though carbon/vacancy binding would be expected to be relaxed, in a disordered grain boundary.

3. Evidence for Carbon Atom/Vacancy Binding in HVEM In-Situ Studies

When foils containing α or α' precipitates formed by quench-aging

were heated in-situ in a high voltage electron microscope, their shrinkage behavior could be followed directly (5). Both α and α' plates exhibited linear shrinkage rates but in different temperature regimes. The α' precipitates dissolved only at a temperature 60-80K higher than that required for the shrinkage of α precipitates and were thus more stable. Assuming diffusion-controlled dissolution the shrinkage rate was proportional to the exponent of an effective stacking fault energy estimated to be near 1500 mJm^{-2} for α precipitates and substantially lower for α' plates. Régnier et al. (8) showed that under electron irradiation above 380 kV carbon atoms were displaced from α precipitates, first generating unfaulted dislocation loops within the platelets and eventually dissolving them completely. Above 500 kV electrons could impart sufficient energy to a carbon atom for it to displace a Pt atom in turn, causing considerable Pt displacement damage in the matrix well below the threshold energy for pure platinum (1300 kV). The effects confirmed the presence of carbon, and the displacement threshold energy of $\sim$95 eV found for the displacement of carbon from α plates points to a strong binding and a large radius of interaction between {001} relaxed vacancies and interstitial carbon atoms.

Electron irradiation was also observed to a have a striking effect near grain boundaries and inclusions in foils used in the membrane diffusion experiments. It was found that an ordered phase with twice the lattice parameter of platinum formed in these regions during electron irradiation above 300 kV in the temperature range from 250 to 600°C (7). Outside of this temperature range disordering

of the radiation-ordered phase took place thermally above 650°C, and athermally (by irradiation above 400 kV) below 250°C.

Small domains of the ordered phase are visible in Fig. 5(a) and a diffraction pattern with superlattice-spots halfway between the matrix spots is seen in Fig. 6b). The simplest structure consistent with this superlattice is the fcc structure, Pt_7C, shown in Fig. 6c. Note that in this structure the carbon atoms occupy substitutional sites or at least occur in tightly bound carbon atom/vacancy pairs whose ordered arrangement is similar to a substitutional occupancy of carbon. This agrees with much earlier X-ray observations of a small lattice shrinkage associated with an ordered phase formed by co-deposition of platinum and carbon from the vapor phase (9).

DISCUSSION

In this review of experimental work on interstitial Pt-C alloys evidence has been shown for a strong binding between carbon and vacancies. The nucleation, growth and dissolution of α, α' and α'' precipitates can only be understood in terms of the co-precipitation of closely bound carbon atom/vacancy pairs. The entire precipitation reaction may be alternatively viewed as the effect of carbon impurities on the recovery of quenched platinum, as the effect of vacancies on the precipitation of carbon or, perhaps most appropriately, as the precipitation of a carbon-vacancy compound in a ternary Pt-C-v alloy. In this view, bound carbon atom/vacancy pairs diffuse and precipitate in a configuration resembling a substitutional atom. This description is even more appropriate in the order/disorder reaction since only minimal relaxation occurs during the ordering of carbon atom/vacancy

pairs to form the Pt_7C phase, whereas their precipitation to form Pt_2C involves the partial collapse of vacancies. Thus, in the ordered phase, C atoms are essentially in substitutional sites even though it is unlikely that they physically reside at the center of their associated vacancy (10).

The reversibility of the order/disorder reaction shows that even in the disordered (or short range ordered) state the carbon remains in solution in a concentration that must be higher than 10 at.-% locally. This exceeds the reported solubility limits for interstitial carbon in platinum by a factor of 10^2 to 10^3. It thus appears that a greatly increased solubility is related to the availability of vacancies. This agrees with the observation that ordered regions were found only in the vicinity of vacancy sources, e.g. grain boundaries and inclusions.

This also provides a possible explanation for the increased size of mounds and pits observed at grain boundaries in the membrane diffusion experiments: interstitial short circuit diffusion along grain boundaries saturates the boundary with carbon; easily produced vacancies combine with carbon atoms and effectively remove them from interstitial solution leading to a region near the boundary with greatly increased concentration of carbon and vacancies. Diffusion in such localized regions would be expected to result in an enhanced vacancy transport.

In the matrix, far from vacancy sources, normal interstitial diffusion dominates and under the assumption of steady-state equilibrium the Lomer equation suggests that only about 1% of all carbon atoms is associated with a vacancy.

Observations supporting this interpretation were made recently in membrane diffusion experiments of hydrogen through aluminum (11). From measurement of the diffusion transient at different temperatures an energy of 0.6 eV was deduced for the binding between H atoms and vacancies. A binding energy of this magnitude is sufficient to cause essentially substitutional diffusion of hydrogen in an intermediate temperature range (350-400° C) whereas normal interstitial diffusion occurred at room temperature.

It appears that a strong binding interaction between interstitial atoms and vacancies in fcc metals is much more common than is usually appreciated. (Of course, this fact is masked by the limited solubility of most fcc metals for interstitial impurities). The magnitude of the binding energy for carbon in platinum and for hydrogen in aluminum suggests that for each a temperature range exists where a substantial fraction of interstitials are bound to vacancies and where a significant vacancy concentration is present in thermal equilibrium. Strong effects on diffusion, segregation, solubility, formation and dissolution of precipitates and ordered phases should also be observable in other interstitial alloys of fcc metals. Finally, it is highly unlikely that a strong interstitial impurity/vacancy binding will not strongly perturb the low temperature recovery spectra in quenching or irradiation experiments on all but the purest materials. Indeed, much of the continuing controversy over the interpretation of recovery stages could stem from the comparison of materials with different and inadequately characterized, interstitial impurity contents.

ACKNOWLEDGEMENT

This work is supported by the Director, Office of Energy Research, Office of Basic Energy Sciences, Materials Sciences Division of the U.S. Department of Energy under Contract No. DE-AC03-76SF00098.

REFERENCES

1. "Point Defects and Defect Interactions in Metals," (1982) Tokyo, Tokyo University Press.
2. K.H. Westmacott and M.I. Perez, J. Nucl. Mat. 83, 231 (1979).
3. M.J. Witcomb, U. Dahmen, K.H. Westmacott, Acta Met. 31, 743 (1983).
4. U. Dahmen, M.J. Witcomb and K.H. Westmacott, Acta Met. 31, 749 (1983).
5. K.H. Westmacott, M.J. Witcomb and U. Dahmen, Acta Met. 31, 755 (1983).
6. P. Ferguson, K.H. Westmacott, R.M. Fisher and U. Dahmen, Mat. Sci. and Technol. 1, 53 (1985).
7. K.H. Westmacott, U. Dahmen and M.J. Witcomb, submitted to Met. Trans. (1985).
8. R.G. Regnier, N.Q. Lam and K.H. Westmacott, Scr. Met 16, 643 (1982), J. Nucl. Mat. 115, 286 (1983).
9. H. Konig, Naturwissenschaften 38, 154 (1951).
10. J.R. Beeler, Jr. in "Interatomic Potentials and Simulation of Lattice Defects," Plenum Press, N.Y. (1972), 339.
11. E. Hashimoto, K. Ono, Y. Murakami and T. Kino in "Point Defects and Defect Interactions in Metals", Univ. of Tokyo Press (1982), p. 496.

FIGURE CAPTIONS

Fig. 1. TEM contrast analysis of α precipitates; with g = <111> (a) displacement contrast is observed but the bounding dislocation is invisible; with g = <220> only two precipitate variants are imaged; both exhibit displacement contrast and the dislocation is in or out of contrast depending on whether $\underline{g}.\underline{b}$ = + 2/3 or - 2/3; with g = <113> (c) two of the variants show the same contrast as in (a), the third shows no displacement contrast but strong dislocation contrast (courtesy Acta Met.).

Fig. 2. TEM contrast analysis of α' precipitates; with g = <111> (a) the precipitates show displacement contrast; with g = <220> (b) one variant is invisible, the others exhibit strong dislocation contrast; with g = <113> (c) the behavior for the two variants is the same as in (a) (courtesy Acta Met.).

Fig. 3. (a) 100 microdiffraction pattern of a single α' platelet edge-on. The carbide spots are streaked (see arrows) and the structure of the Pt_2C carbide is shown in (b).

Fig. 4. Contrast analysis of α'' precipitates (marked A) with displacement vector a [010]. Under all conditions except $\underline{g}.\underline{b}$ = 0 the precipitates exhibit no (or faint residual) displacement contrast and strong dislocation contrast. (courtesy Acta Met.).

Fig. 5. Scanning electron micrographs of (a) outer, decarburized surface and (b) inner, carburized surface of a Pt foil subjected to a carbon flux at 900° C. Note pits and mounds on decarburized (a)

and carburized (b) side, respectively.

Fig. 6. (a) Dark field image showing ordered domains in region near a grain boundary; (b) corresponding selected area diffraction pattern with superlattice spots; (c) fcc structure of Pt_7C, the simplest structure consistent with the diffraction evidence.

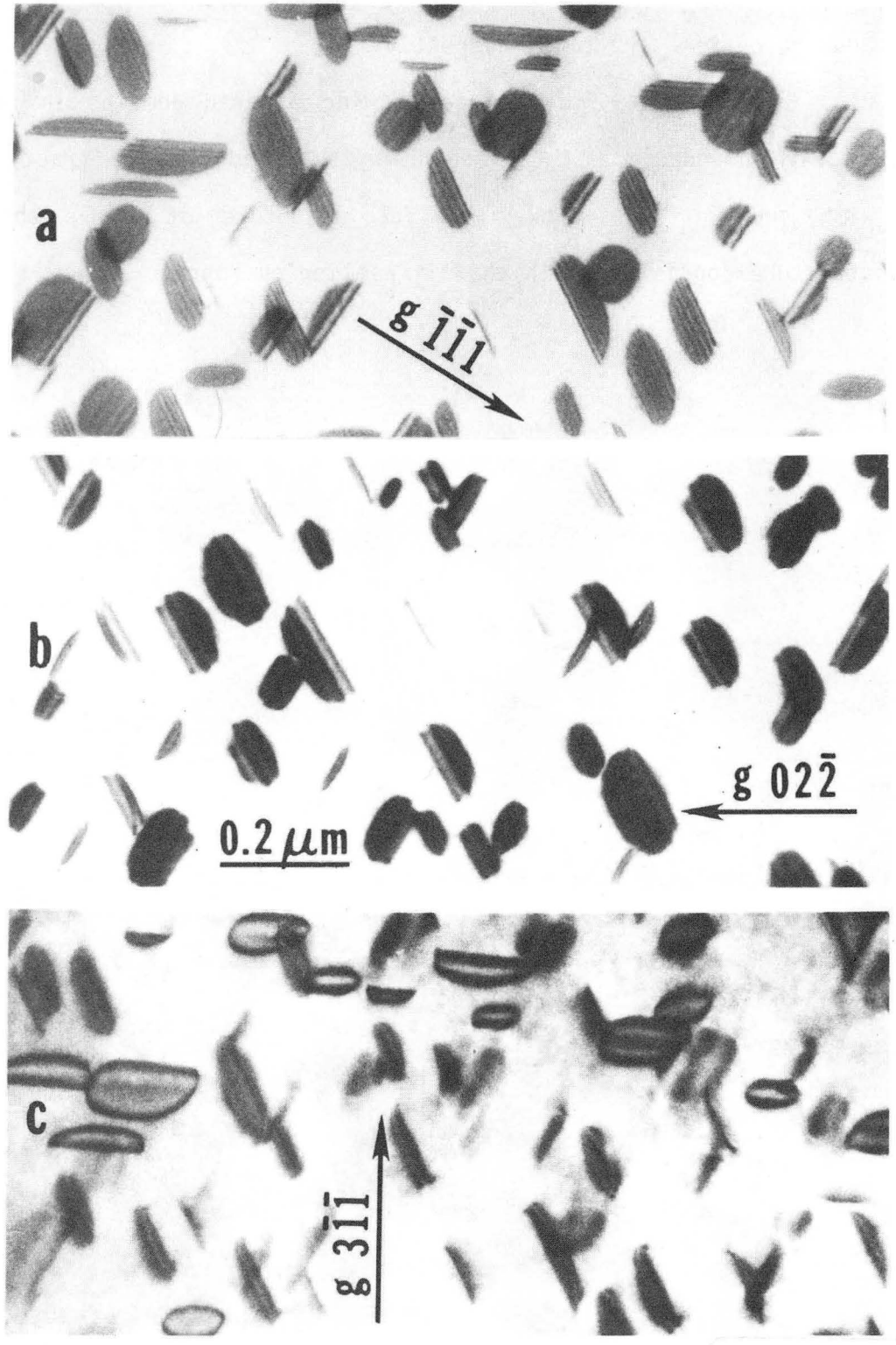

XBB 827-5936

Fig. 1.

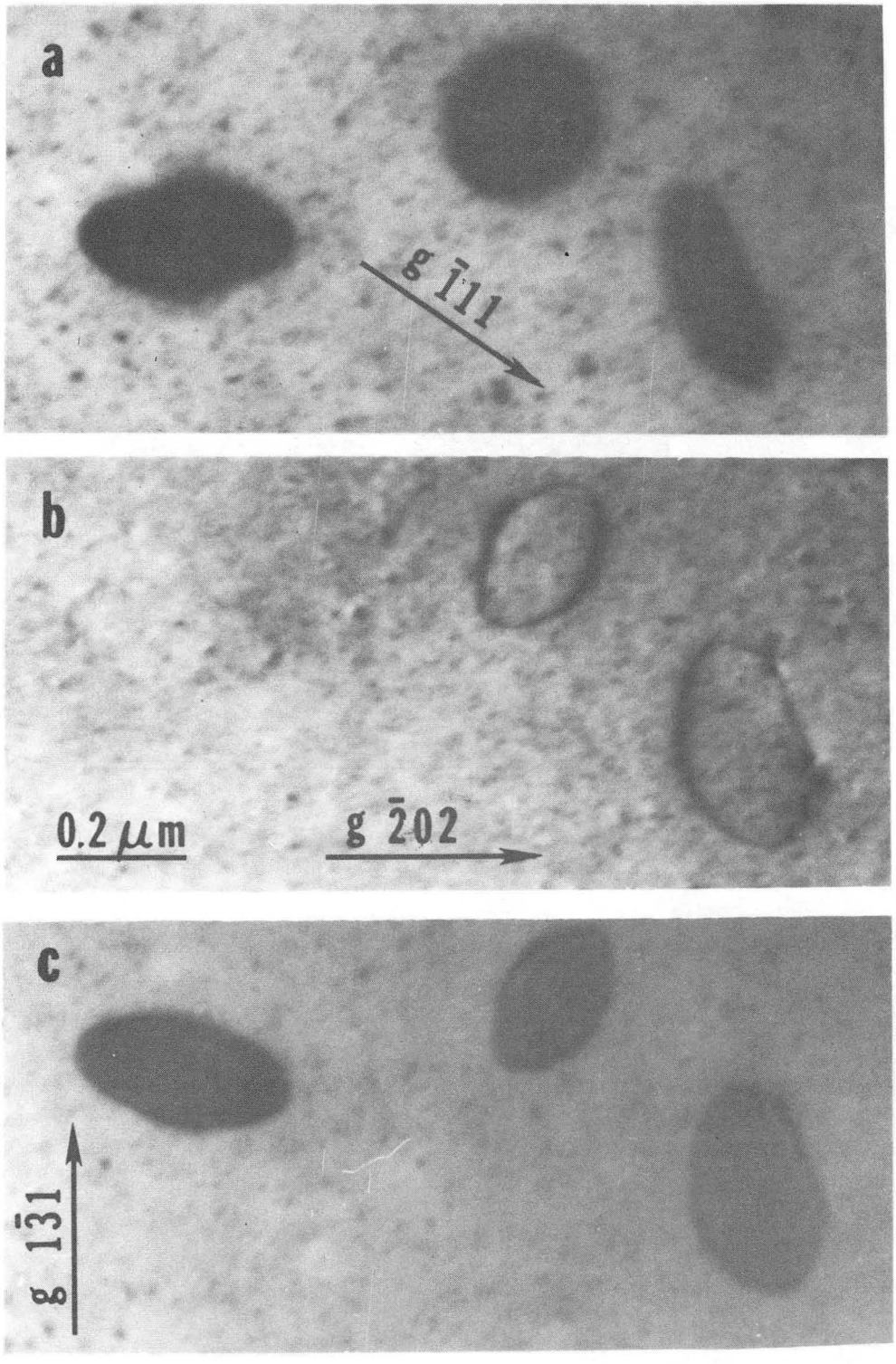

XBB 827-5934

Fig. 2.

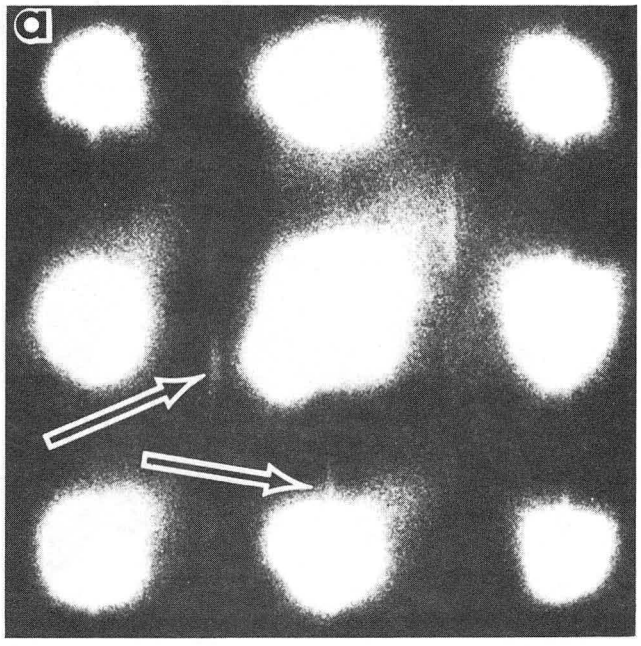

XBB 858-6521

Fig. 3(a).

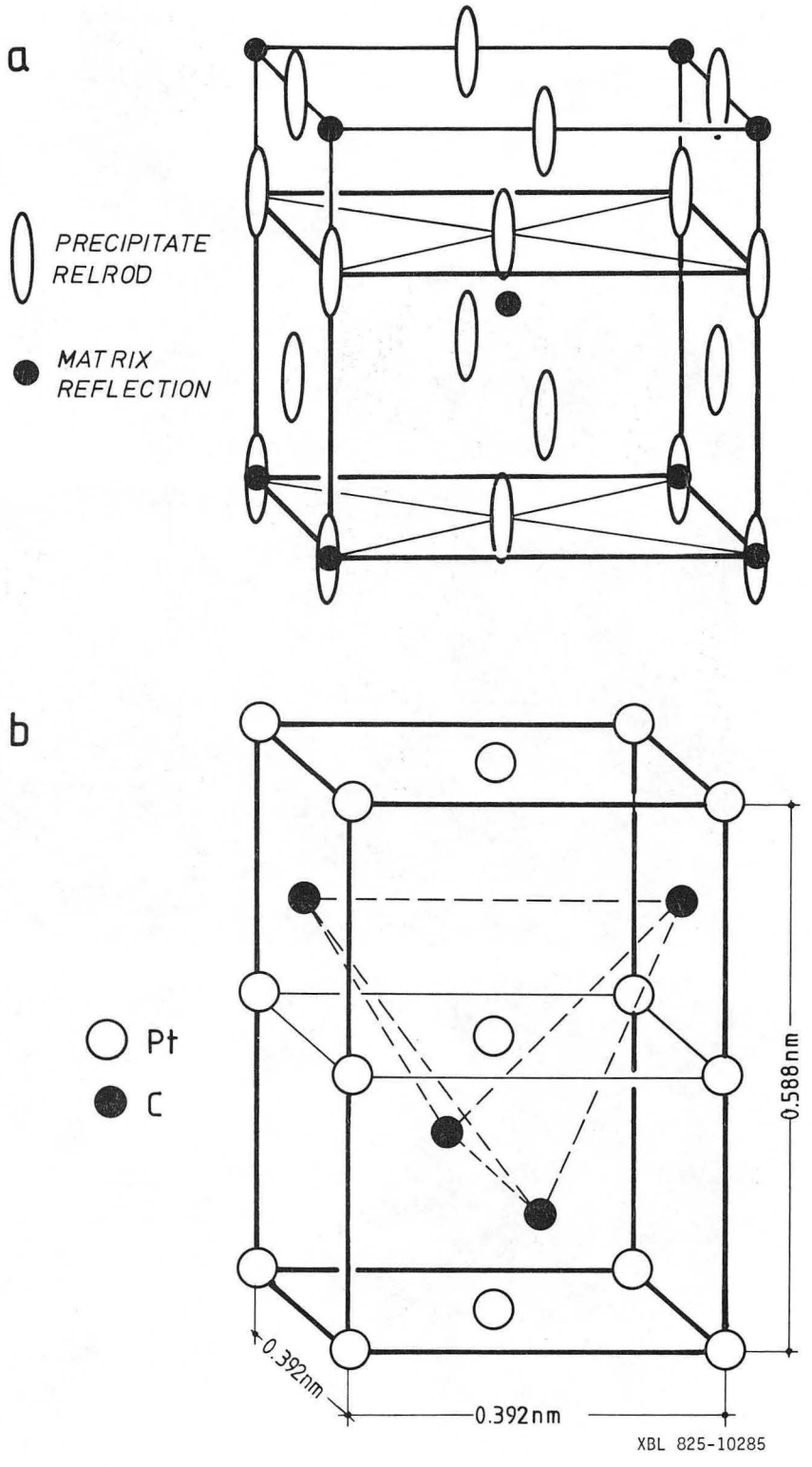
a
PRECIPITATE RELROD
MATRIX REFLECTION
b
Pt
C
0.588nm
0.392nm
0.392nm
XBL 825-10285

Fig. 3(b).

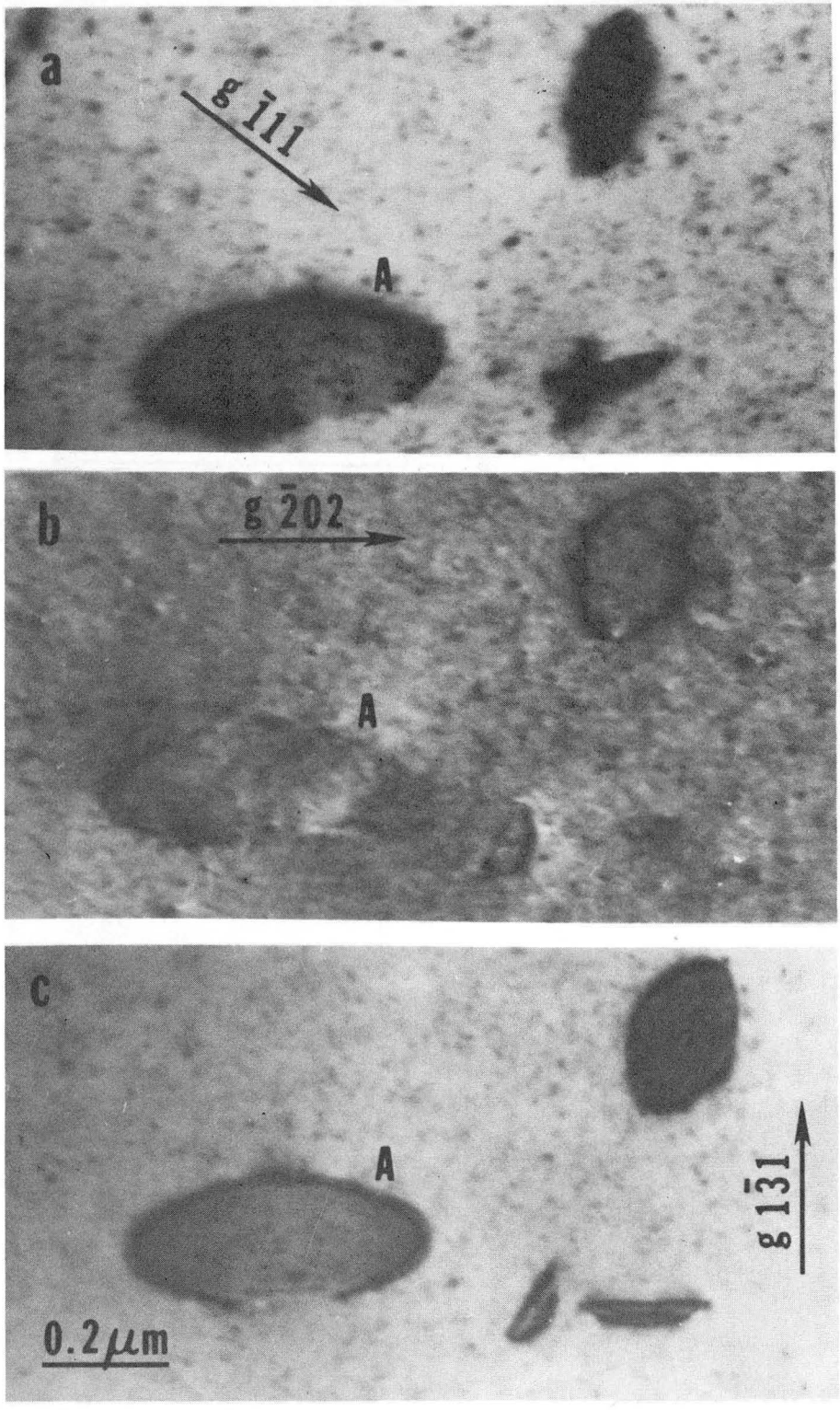

XBB 827-5933

Fig. 4.

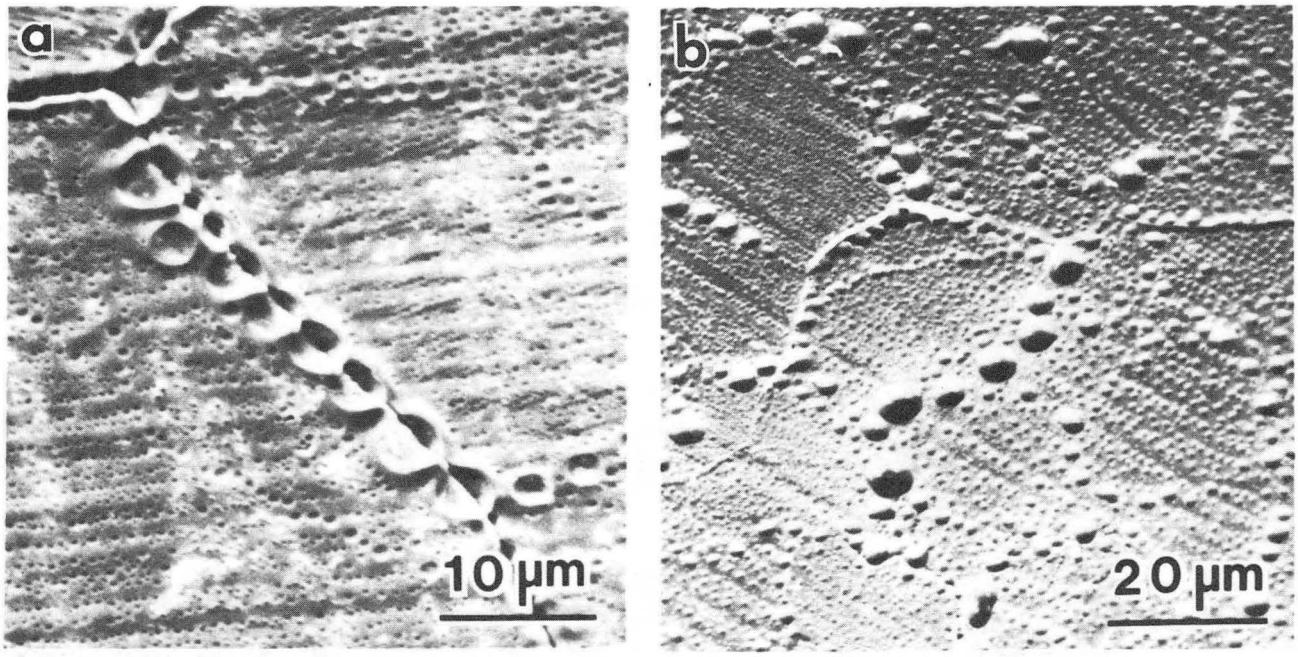

XBB 858-6522

Fig. 5(a,b).

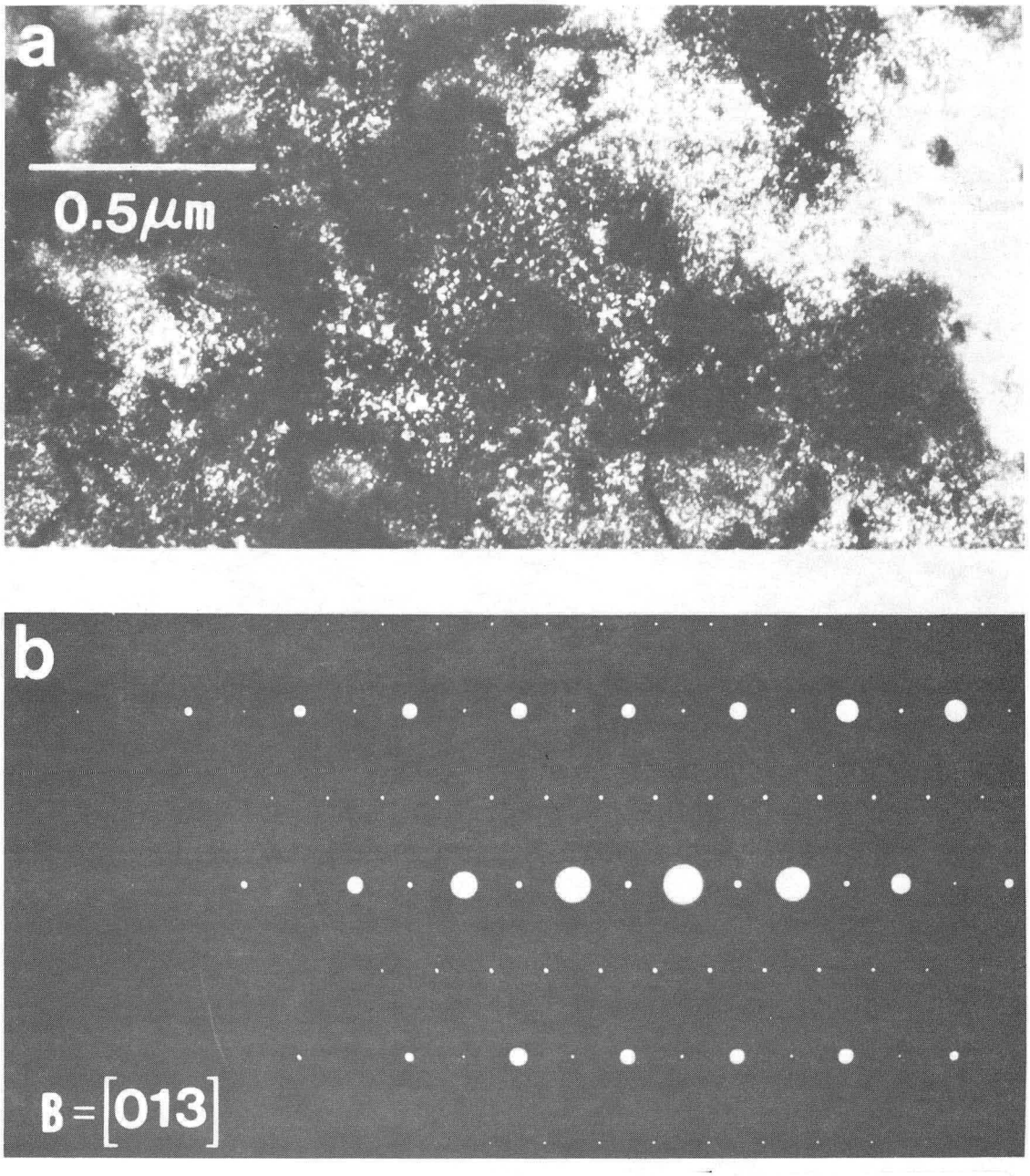

XBB 856-4260

Fig. 6(a,b)

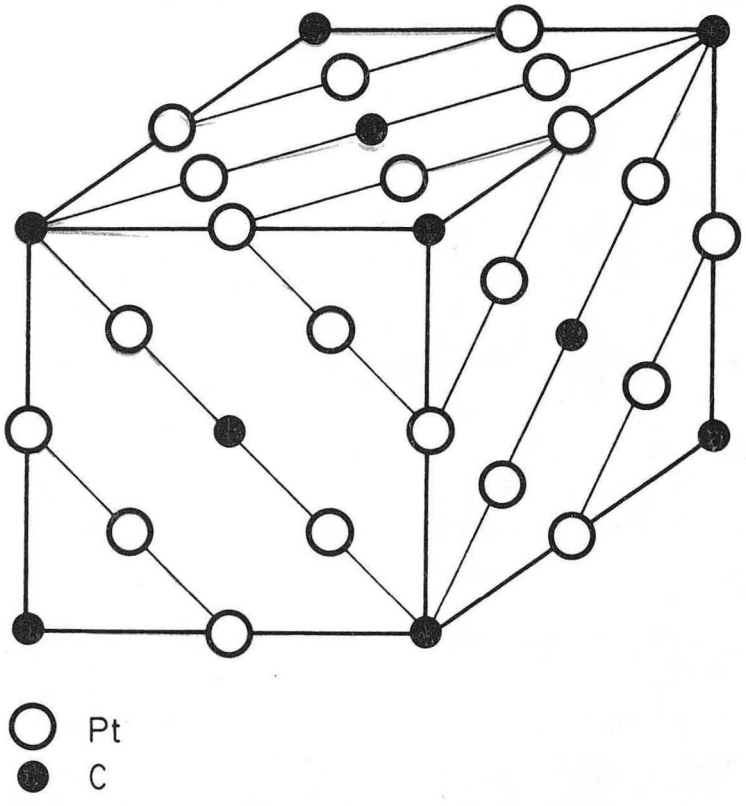

XBL 854-2220

Fig. 6(c)

LAWRENCE BERKELEY LABORATORY
TECHNICAL INFORMATION DEPARTMENT
UNIVERSITY OF CALIFORNIA
BERKELEY, CALIFORNIA 94720